

Recognition of 1,3-Butadiene by a Porous Coordination Polymer

Keisuke Kishida, Yoshikuni Okumura,* Yoshihiro Watanabe, Megumi Mukoyoshi, Silvia Bracco, Angiolina Comotti, Piero Sozzani, Satoshi Horike,* and Susumu Kitagawa*

Abstract: The separation of 1,3-butadiene from C_4 hydrocarbon mixtures is imperative for the production of synthetic rubbers, and there is a need for a more economical separation method, such as a pressure swing adsorption process. With regard to adsorbents that enable C_4 gas separation, $[Zn(NO_2ip)(dpe)]_n$ (SD-65; NO_2ip = 5-nitroisophthalate, dpe = 1,2-di(4-pyridyl)ethylene) is a promising porous material because of its structural flexibility and restricted voids, which provide unique guest-responsive accommodation. The 1,3-butadiene-selective sorption profile of SD-65 was elucidated by adsorption isotherms, in situ PXRD, and SSNMR studies and was further investigated by multigas separation and adsorption-desorption-cycle experiments for its application to separation technology.

1,3-Butadiene is a major industrial chemical used in the production of synthetic rubbers. It is typically produced through extractive distillation from C_4 hydrocarbons because of the similarity of isomers (see Table S1 in the Supporting Information).^[1] The extractive distillation requires large amounts of energy through the reboiling of 1,3-butadiene in organic solvents. An alternative energy-efficient purification method is pressure swing adsorption (PSA) with microporous adsorbents that can separate gas molecules thermodynamically or kinetically.^[2] The former thermodynamic approach uses adsorbents containing accessible cations, such as Ag^+ and Cu^+ ,^[3] thus enabling π -complexation to 1,3-butadiene for separation; however, it requires time and energy to regenerate the adsorbent under ambient conditions. The latter kinetic, size-selective separation, for example, with all-silica decadecasil 3R (DD3R), has also been unsuccessful in separating 1,3-butadiene from *trans*-2-butene because of their

similar molecular size.^[4] Thus, adsorbents that satisfy both 1,3-butadiene selectivity and regeneration ability are required.

Porous coordination polymers (PCPs) or metal-organic frameworks (MOFs) have attracted considerable attention because of their structural diversity.^[5] Although many PCPs have been proposed for separating olefin/paraffin mixtures,^[6] all focus on identifying a mono-olefin from paraffin.^[7] No reports have appeared on the separation of C_4 diolefins from mono-olefins and paraffin. Because of the significance of separating 1,3-butadiene and consequent chemical processes, we describe herein the first example of a PCP for the separation of 1,3-butadiene from six major C_4 hydrocarbons, including four mono-olefins, at ambient temperature and pressure.

We employed $[Zn(NO_2ip)(dpe)]_n$ (SD-65; NO_2ip = 5-nitroisophthalate, dpe = 1,2-di(4-pyridyl)ethylene), as it possesses thermodynamic-based structural flexibility.^[8] Through coordination with two isophthalate and two dipyridyl ligands with tetrahedral geometry, Zn^{2+} forms pseudodiamondoid frameworks, as depicted in Figure 1 a. These frameworks are triply interpenetrated and form a flexible, dense coordination

[*] Dr. K. Kishida, Dr. Y. Okumura, Y. Watanabe, M. Mukoyoshi
Institute for Advanced and Core Technology, Showa Denko K.K.
2 Oaza Nakanos, Oita 870-0189 (Japan)
E-mail: okumura.yoshikuni.xhmlr@showadenko.com
Dr. S. Horike, Prof. S. Kitagawa
Department of Synthetic Chemistry and Biological Chemistry
Graduate School of Engineering, Kyoto University
Katsura, Nishikyo-ku, Kyoto 615-8510 (Japan)
E-mail: horike@sbchem.kyoto-u.ac.jp
kitagawa@icems.kyoto-u.ac.jp

Prof. S. Kitagawa
Institute for Integrated Cell-Material Sciences (WPI-iCeMS)
Kyoto University
Yoshida, Sakyo-ku, Kyoto 606-8501 (Japan)

Dr. S. Bracco, Prof. A. Comotti, Prof. P. Sozzani
Department of Materials Science, University of Milano Bicocca
Via R. Cozzi 55, 20125 Milan (Italy)

Supporting information for this article can be found under:
<http://dx.doi.org/10.1002/anie.201607676>.

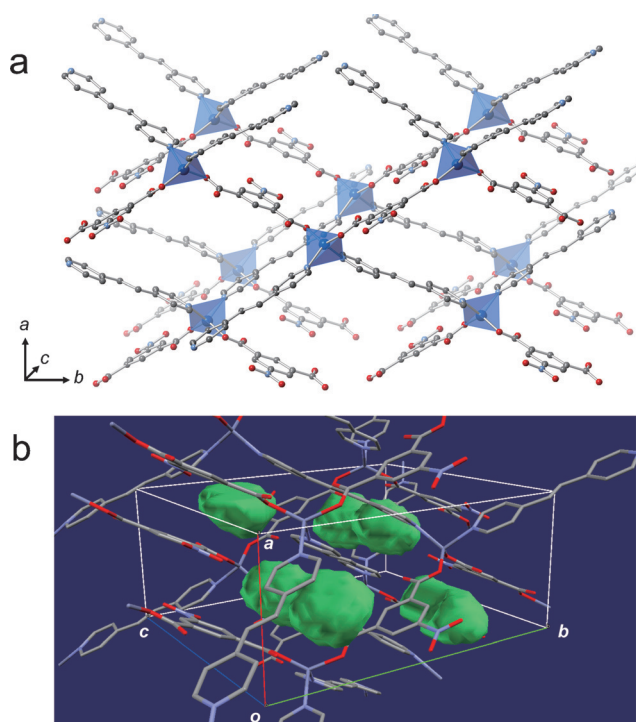


Figure 1. a) Pseudodiamondoid network of SD-65 along the c axis. Blue polyhedra and red, blue, and gray spheres represent Zn, O, N, and C atoms, respectively. b) Isolated voids (green spheres) in the SD-65 unit cell. The probe radius for the calculation is 1.3 Å.

polymer with discrete, isolated voids (Figure 1b). Each void has a volume of 45 \AA^3 ,^[9] and is located in the interspaces of the entangled networks.

Single-component gas-adsorption studies of seven C_4 hydrocarbons (see Table S1) at 25°C revealed specific 1,3-butadiene sorption behavior of SD-65. The uptake of all butenes and butanes on SD-65 was less than $2.5 \text{ cm}^3 \text{ g}^{-1}$ at 101 kPa and 25°C (Figures 2a,b). However, the uptake of 1,3-

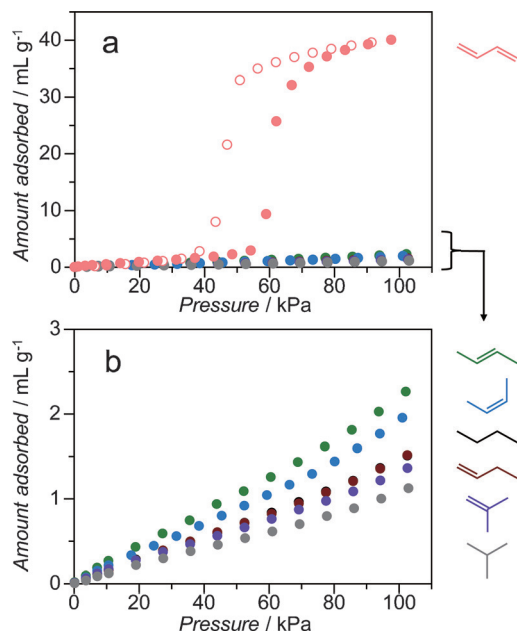


Figure 2. a) Adsorption isotherms of SD-65 for 1,3-butadiene (pink; open circles show the desorption isotherm), *trans*-2-butene (green), *cis*-2-butene (blue), *n*-butane (black), 1-butene (brown), isobutene (purple), and isobutane (gray) at 25°C . b) Enlarged graph from 0 to 3 mL g^{-1} of amount adsorbed.

butadiene was $40 \text{ cm}^3 \text{ g}^{-1}$ at 101 kPa with a sigmoid-type sorption profile; adsorption began at 60 kPa, whereas desorption began at 50 kPa. This profile is referred to as a gate-opening phenomenon and represents the flexible nature of SD-65.^[10] It suggests that 1,3-butadiene sorption stems from the structural flexibility of the framework. We also investigated selected C_4 adsorption isotherms of NaX zeolite and four PCPs with flexible and nonflexible structures (Figure 3). The studied PCPs were $[\text{Zn}(\text{2-methylimidazolate})_2]$ (Zn-ZIF-8),^[11] $[\text{Al}(\text{OH})(1,4\text{-benzenedicarboxylate})]$ (Al-MIL-53),^[12] $[\text{Zn}_2(\text{fumarate})_2(4,4'\text{-bpy})]$,^[13] and $[\text{Ca}(\text{squarate})(\text{H}_2\text{O})]$.^[14] NaX zeolite, Zn-ZIF-8, and Al-MIL-53 (Figure 3a–c) adsorbed not only 1,3-butadiene but also *n*-butane and 1-butene with Type-I profiles, thus indicating that these pores are too large to accommodate 1,3-butadiene in such a way that it can be differentiated from butanes and butenes. Flexible $[\text{Zn}_2(\text{fumarate})_2(4,4'\text{-bpy})]$ absorbed 1,3-butadiene with a Type-1 profile at 25°C (Figure 3d). Although this compound did not adsorb *n*-butane, it started to adsorb 1-butene at 30 kPa with a gate-opening profile, thus indicating that the pore opening is still too large to recognize 1,3-butadiene selectively in the presence of butenes. $[\text{Ca}(\text{squarate})(\text{H}_2\text{O})]$ has a rigid

and ultra-microporous structure with pore openings of $3.4 \times 3.4 \text{ \AA}^2$ and showed adsorption profiles for *trans*-2-butene and 1,3-butadiene well above those of the other five C_4 gases (Figure 3e). The observed distinct isotherms originate from a molecular-sieving effect, like that observed for zeolite ZSM-5^[2b] and DD3R;^[4a] the inherent similarity of *trans*-2-butene and 1,3-butadiene makes the separation unfeasible by the molecular-sieving effect. These results indicate that SD-65 is the best candidate because of its restricted voids and structural flexibility. On the other hand, the single-component gas adsorption isotherms for such soft frameworks do not always correlate with their performance in the separation of gas mixtures. A study on the ability of SD-65 to separate gas mixtures is discussed below.

To investigate the structural rearrangement, we measured the powder X-ray diffraction (PXRD) patterns of SD-65 under variable pressure of 1,3-butadiene (Figure 4). In situ PXRD studies revealed gradual, crystal-to-crystal structural transformation upon 1,3-butadiene adsorption. During the adsorption process, some diffraction peaks diminished, and new diffraction peaks emerged that could not be indexed to either the same unit cell or a combination of unit cells SD-65 without guest molecules. However, the comparison of the PXRD pattern with that of an isorecticular compound, $[\text{Zn}(\text{NO}_2\text{ip})(\text{dpa})]_n$ ($\text{dpa} = 1,2\text{-di}(4\text{-pyridyl})\text{ethane}$),^[15] allowed us to establish that the framework of SD-65 expanded along the *a* axis and contracted along the *b* axis upon 1,3-butadiene sorption in a reversible manner (see Figures S1 and S2 in the Supporting Information).

The structural transformation was also apparent by ^{13}C MAS NMR spectroscopy: A generalized change in chemical shift was observed in SD-65 after loading with $[\text{D}_6]1,3\text{-butadiene}$ at 96 kPa and room temperature, which corresponds to the virtually complete filling of the cavities (Figure 5). In particular, the downfield shift of C4 (Figure 5b) is consistent with a deviation from an *s-cis* planar conformation of the C3–C6 bond of dpe in the presence of butadiene. The use of hydrogen-depleted perdeuterobutadiene highlights the efficient magnetization transfer from the host hydrogen atoms to the guest CD and CD_2 carbon atoms in cross-polarization experiments, thus indicating short intermolecular distances (Figure 5b). Whereas the 2D ^1H – ^{13}C HETCOR NMR spectrum at a contact time of $50 \mu\text{s}$ enabled the assignment of host proton signals (Figure 5e), the 2D NMR spectrum at a contact time of 0.5 ms indicates that the H5 hydrogen atom *ortho* to the nitrogen atom of the pyridyl moiety ($\delta = 8.2 \text{ ppm}$) correlates with the CD_2 carbon atoms ($\delta = 113.7 \text{ ppm}$), thus unambiguously showing the close proximity of these atoms in the host–guest structure (Figure 5d).

At a longer contact time of 2 ms, the H4 atoms participate in the same spin system H5-CD_2 , thus confirming that the CD_2 group selectively interacts with one side edge of the pyridyl ring (Figure 5c). At this contact time, the CD carbon atom receives the magnetization from the nitroisophthalate benzene H10 atom resonating at $\delta = 8.9 \text{ ppm}$. Such a high ^1H chemical-shift value indicates an acidic aromatic proton, which can favorably interact with the electron-rich system of butadiene (Figure 5g). The tight fitting of butadiene in the

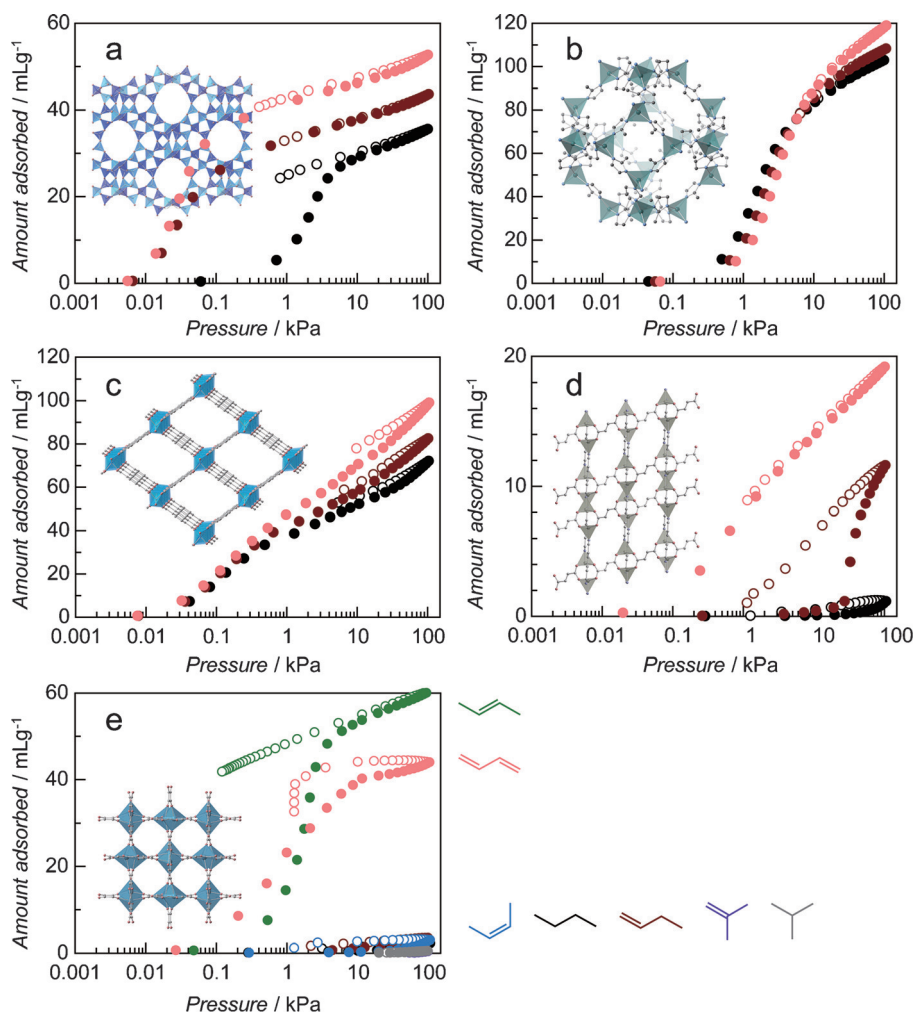


Figure 3. Isotherms of adsorption (solid circles) and desorption (open circles) at 25 °C on a) NaX zeolite, b) [Zn(2-methylimidazolate)₂] (Zn-ZIF-8), c) [Al(OH)(1,4-benzenedicarboxylate)] (Al-MIL-53), d) [Zn₂(fumarate)₂(4,4'-bpy)] (pink: 1,3-butadiene, brown: 1-butene, black: *n*-butane), and e) [Ca(squarate)(H₂O)] (green: *trans*-2-butene, blue: *cis*-2-butene, purple: isobutene, and gray: isobutane are also shown).

cavity suggests restricted mobility of the guest in the structure, which is consistent with the long ¹³C *T*₁ spin–lattice relaxation times of more than 150 s and a quasi-static arrangement of the C–D bonds, as confirmed by ²H spin-echo NMR spectroscopy (see Figures S8–S11)^[16]

We further measured the adsorption isotherms at various temperatures to obtain insight into the flexibility-based separation of 1,3-butadiene (see Figure S3). The gate-opening pressure for 1,3-butadiene decreased with decreasing operating temperature. The amount adsorbed at 0 °C and 97 kPa reached 52 cm³ g^{−1}, which corresponds to one molecule per void in the structure in Figure 1b. However, the volume of each void (45 Å³) is smaller than the van der Waals volume of 1,3-butadiene (70 Å³).^[17] SD-65 transforms its structure in such a way that 1,3-butadiene diffuses into the isolated, small voids and is accommodated there. The isosteric heat for 1,3-butadiene from the Clausius–Clapeyron equation is 40 kJ mol^{−1} (see Figure S4), which is significantly smaller than that of the Ag⁺-containing zeolite Y (100–

122 kJ mol^{−1})^[3b] and identical to that of the charge-neutral zeolite DD3R (39 kJ mol^{−1}).^[18] The difference in the interaction between the adsorbent and C₄ hydrocarbons would be derived mainly from the difference in quadrupole moment of these gaseous molecules; −5.5 D Å for 1,3-butadiene, −2.3 D Å for *trans*-2-butene, and −1.9 D Å for 1-butene. The larger quadrupole moment of 1,3-butadiene exclusively induces a structural change of the framework and is small enough for diffusion into the voids, thus leading to the accommodation of 1,3-butadiene in SD-65.

Besides gas adsorption, regeneration of the adsorbent is another important factor for applicability in PSA systems. Figure 6a shows the results of a pressure swing adsorption–desorption cyclic study of SD-65 with 1,3-butadiene at 25 °C (see Figure S5). The 1,3-butadiene adsorption capacity of SD-65 for the first run was 26 cm³ g^{−1} at 125 kPa and 25 °C for 5 min. Minimal deterioration in the adsorption capacity was detected during four cycles of measurement, thus indicating good regeneration ability of SD-65 for 1,3-butadiene. The regeneration ability is good because the accommodation is based only on weak adsorbent–adsorbate interactions. Conversely, a repeated sorption study for NaX zeolite, Na₈₆[(AlO₂)₈₆(SiO₂)₁₀₆], revealed a significant decrease in the amount adsorbed from 48 cm³ g^{−1} in the first run to 10 cm³ g^{−1} in the second run. These results suggest a strong interaction between the 1,3-butadiene molecules and the cationic framework of the zeolite, and thus demonstrate the advantage of flexible PCPs over traditional adsorbents for separating 1,3-butadiene in a PSA process with regard to the small energy of adsorption.

The 1,3-butadiene selectivity of SD-65 was examined by a breakthrough experiment with a C₄ hydrocarbon mixture (Figure 6b; see also Figures S6 and S7). We used crushed pellets of SD-65 to reduce the dead volume in the apparatus and avoid an unnecessary pressure drop in the measurement. As the gas mixture, we employed a C₄ fraction comprising 1,3-butadiene (40%), a butene mixture (49%), and a butane mixture (11%). The breakthrough curves at 25 °C and 230 kPa showed 1,3-butadiene-selective sorption profiles, while the outlet gas contained unadsorbed 1,3-butadiene at the breakthrough point because of low 1,3-butadiene uptake in the low-pressure region. The dead volume between the

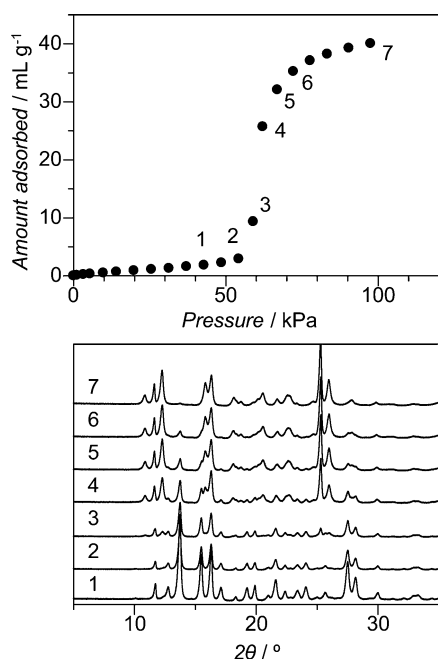


Figure 4. In situ PXRD patterns at each equilibrium point of 1,3-butadiene adsorption on SD-65 at 25 °C.

PCP sample tube and the gas chromatograph led to breakthrough curves in which the gas flow rates started from non-zero rates. The insufficient signal/noise ratio for each profile is due to the scale of our apparatus, and improvement of the ratio would require larger-scale evaluation. However, after the breakthrough point, the calculated outflow rates of butenes and butanes reached the inflow rates of those gases, and the outflow rate of 1,3-butadiene kept increasing, thus indicating no replacement of adsorbed butenes and butanes by 1,3-butadiene, and slow but selective sorption of 1,3-butadiene from the C_4 gas mixture. A material-balance calculation based on the saturation conditions, at 180 min, revealed that the amount of 1,3-butadiene, butenes, and butanes adsorbed on SD-65 were 28, 6, and $0.4 \text{ cm}^3 \text{ g}^{-1}$, respectively, and that the 1,3-butadiene selectivity was 6.6.^[8] With this hydrophobic character, the preferential adsorption of 1,3-butadiene from the C_4 fraction and low energy consumption for the regeneration of SD-65 are promising characteristics for application in naphtha crackers.

In conclusion, we have developed an adsorbent-based separation of 1,3-butadiene from a C_4 hydrocarbon mixture under ambient conditions by using a triply interpenetrated flexible PCP, SD-65, containing discrete voids. By considering the crystal structures and adsorption behavior of SD-65, we deduced that specially isolated voids of SD-65 selectively captured 1,3-butadiene molecules by expanding their overall structure and excluding other C_4 hydrocarbons. Despite the small difference in the physical properties of C_4 hydrocarbons, SD-65 can separate 1,3-butadiene from C_4 hydrocarbon mixtures and readily release adsorbed 1,3-butadiene under the expected PSA conditions. From the viewpoint of materials design for specific gas separation under ambient conditions, the results of this study suggest that the key is to combine both

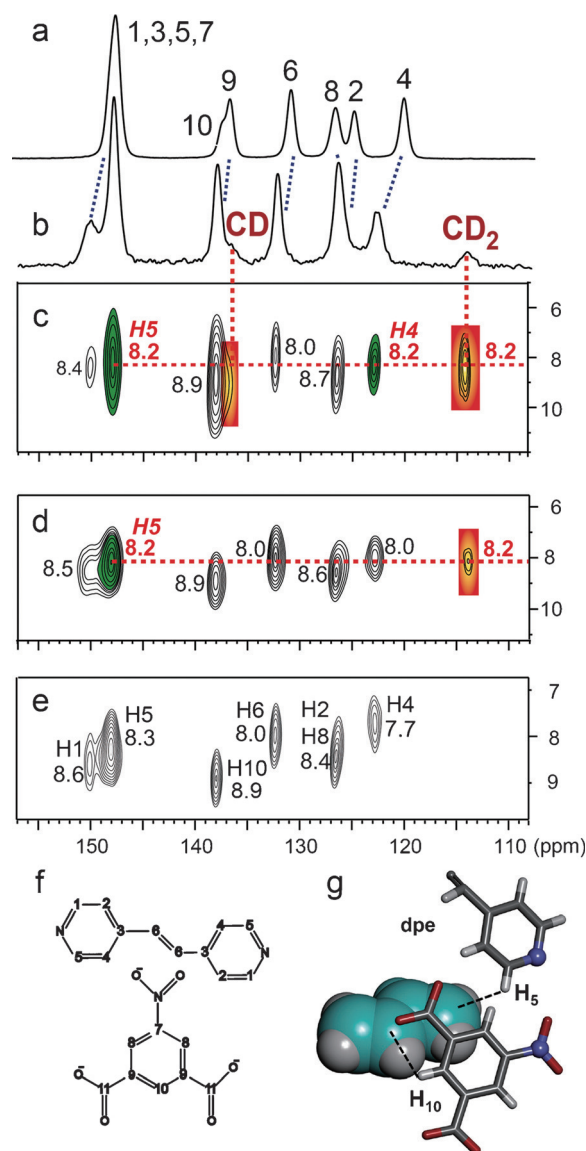


Figure 5. a, b) ^{13}C CP MAS NMR spectra of SD-65 (a) and SD-65 accommodating $[\text{D}_6]1,3\text{-butadiene}$ (b). c–e) 2D $^1\text{H}\text{--}^{13}\text{C}$ HETCOR spectra of SD-65/ $[\text{D}_6]1,3\text{-butadiene}$ at 2 ms (c), 0.5 ms (d), and 0.05 ms (e). f) Numbering of chemical structures. g) Intermolecular interactions between the host and the guest.

narrow voids and structural flexibility for the separation of light gas mixtures.

Acknowledgements

This research was partially supported by the New Energy and Industrial Technology Development Organization (NEDO) and a Grant-in-Aid for Young Scientists (A) from the Japan Society for the Promotion of Science. We acknowledge Dr. Ryotaro Matsuda and Dr. Hiroshi Sato for measuring in situ XRPD and Dr. M. Negroni for assistance with MAS NMR spectroscopy.

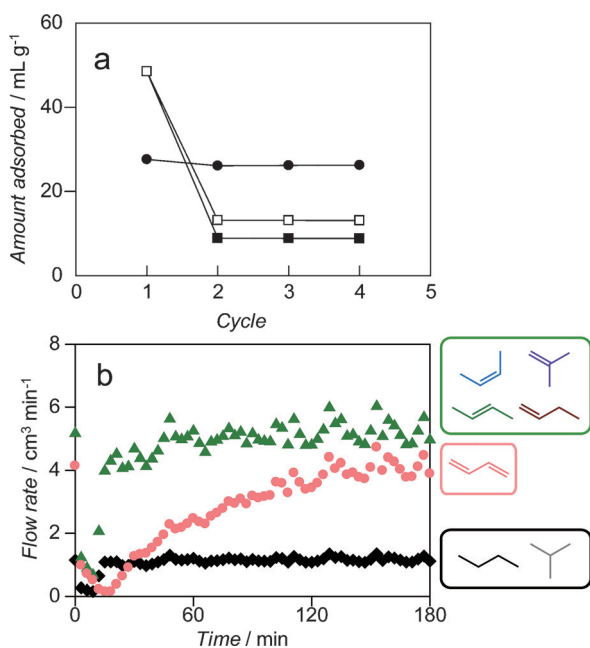


Figure 6. a) Cycle tests of 1,3-butadiene adsorption (125 kPa for 5 min) and desorption (at 25 °C below 1 kPa for 1 min or for 60 min: desorption from SD-65 for 1 min (solid circles) and from NaX zeolite for 1 min (solid squares) or 60 min (open squares)). b) Breakthrough curves of 1,3-butadiene (pink circles), butenes (green triangles: 1-butene, 2-butenes, and isobutene), and butanes (black diamonds: *n*-butane and isobutene) on SD-65 at 25 °C with a total pressure of 230 kPa and a total flow rate of 10 cm³ min⁻¹.

Keywords: gas separation · host–guest systems · microporous materials · molecular recognition · coordination polymers

How to cite: *Angew. Chem. Int. Ed.* **2016**, *55*, 13784–13788
Angew. Chem. **2016**, *128*, 13988–13992

- [1] U. Wagner, H. M. Weitz, *Ind. Eng. Chem.* **1970**, *62*, 43–48.
- [2] a) S. Sircar, *Ind. Eng. Chem. Res.* **2006**, *45*, 5435–5448; b) R. T. Yang, *Gas Separation by Adsorption Processes*, Imperial College Press, London, **1997**.
- [3] a) J. Padin, R. T. Yang, C. L. Munson, *Ind. Eng. Chem. Res.* **1999**, *38*, 3614–3621; b) A. Takahashi, R. T. Yang, C. L. Munson, D. Chinn, *Ind. Eng. Chem. Res.* **2001**, *40*, 3979–3988; c) A. Takahashi, R. T. Yang, C. L. Munson, D. Chinn, *Langmuir* **2001**, *17*, 8405–8413; d) J. W. Priegnitz, U.S. Patent, Vol. 3,992,471, Nov 16, 1976, **1976**.
- [4] a) J. Gascon, W. Blom, A. van Miltenburg, A. Ferreira, R. Berger, F. Kapteijn, *Microporous Mesoporous Mater.* **2008**, *115*, 585–593; b) C. Gücüyener, J. van den Bergh, A. M. Joaristi, P. C. M. Magusin, E. J. M. Hensen, J. Gascon, F. Kapteijn, *J. Mater. Chem.* **2011**, *21*, 18386.
- [5] a) M. Eddaoudi, D. B. Moler, H. Li, B. Chen, T. M. Reineke, M. O’Keeffe, O. M. Yaghi, *Acc. Chem. Res.* **2001**, *34*, 319–330; b) S. Kitagawa, R. Kitaura, S. Noro, *Angew. Chem. Int. Ed.* **2004**, *43*, 2334–2375; *Angew. Chem.* **2004**, *116*, 2388–2430; c) G. Férey, *Chem. Soc. Rev.* **2008**, *37*, 191–214; d) J. R. Li, R. J. Kuppler, H. C. Zhou, *Chem. Soc. Rev.* **2009**, *38*, 1477–1504; e) K. Sumida, D. L. Rogow, J. A. Mason, T. M. McDonald, E. D. Bloch, Z. R. Herm, T. H. Bae, J. R. Long, *Chem. Rev.* **2012**, *112*, 724–781; f) R. B. Getman, Y. S. Bae, C. E. Wilmer, R. Q. Snurr, *Chem. Rev.* **2012**, *112*, 703–723; g) J. Canivet, A. Fateeva, Y. Guo, B. Coasne, D. Farrusseng, *Chem. Soc. Rev.* **2014**, *43*, 5594–5617; h) A. Schneemann, V. Bon, I. Schwedler, I. Senkovska, S. Kaskel, R. A. Fischer, *Chem. Soc. Rev.* **2014**, *43*, 6062–6096.
- [6] Y. He, R. Krishna, B. Chen, *Energy Environ. Sci.* **2012**, *5*, 9107.
- [7] a) Z. Bao, S. Alnemrat, L. Yu, I. Vasiliev, Q. Ren, X. Lu, S. Deng, *Langmuir* **2011**, *27*, 13554–13562; b) J. van den Bergh, C. Gücüyener, E. A. Pidko, E. J. Hensen, J. Gascon, F. Kapteijn, *Chem. Eur. J.* **2011**, *17*, 8832–8840; c) Y. S. Bae, C. Y. Lee, K. C. Kim, O. K. Farha, P. Nickias, J. T. Hupp, S. T. Nguyen, R. Q. Snurr, *Angew. Chem. Int. Ed.* **2012**, *51*, 1857–1860; *Angew. Chem.* **2012**, *124*, 1893–1896; d) U. Böhme, B. Barth, C. Paula, A. Kuhnt, W. Schwieger, A. Mundstock, J. Caro, M. Hartmann, *Langmuir* **2013**, *29*, 8592–8600; e) S. J. Geier, J. A. Mason, E. D. Bloch, W. L. Queen, M. R. Hudson, C. M. Brown, J. R. Long, *Chem. Sci.* **2013**, *4*, 2054; f) B. Li, Y. Zhang, R. Krishna, K. Yao, Y. Han, Z. Wu, D. Ma, Z. Shi, T. Pham, B. Space, J. Liu, P. K. Thallapally, J. Liu, M. Chrzanowski, S. Ma, *J. Am. Chem. Soc.* **2014**, *136*, 8654–8660.
- [8] S. Horike, K. Kishida, Y. Watanabe, Y. Inubushi, D. Umeyama, M. Sugimoto, T. Fukushima, M. Inukai, S. Kitagawa, *J. Am. Chem. Soc.* **2012**, *134*, 9852–9855.
- [9] A. L. Spek, *Acta Crystallogr. Sect. D* **2009**, *65*, 148–155.
- [10] S. Horike, S. Shimomura, S. Kitagawa, *Nat. Chem.* **2009**, *1*, 695–704.
- [11] a) X. C. Huang, Y. Y. Lin, J. P. Zhang, X. M. Chen, *Angew. Chem. Int. Ed.* **2006**, *45*, 1557–1559; *Angew. Chem.* **2006**, *118*, 1587–1589; b) K. S. Park, Z. Ni, A. P. Côté, J. Y. Choi, R. Huang, F. J. Uribe-Romo, H. K. Chae, M. O’Keeffe, O. M. Yaghi, *Proc. Natl. Acad. Sci. USA* **2006**, *103*, 10186–10191.
- [12] T. Loiseau, C. Serre, C. Huguenard, G. Fink, F. Taulelle, M. Henry, T. Bataille, G. Férey, *Chem. Eur. J.* **2004**, *10*, 1373–1382.
- [13] B. Q. Ma, K. L. Mulfort, J. T. Hupp, *Inorg. Chem.* **2005**, *44*, 4912–4914.
- [14] C. Robl, A. Weiss, *Mater. Res. Bull.* **1987**, *22*, 373–380.
- [15] M. Arıcı, O. Z. Yeşilel, S. Keskin, O. Şahin, *J. Solid State Chem.* **2014**, *210*, 280–286.
- [16] a) A. Comotti, S. Bracco, T. Ben, S. Qiu, P. Sozzani, *Angew. Chem. Int. Ed.* **2014**, *53*, 1043–1047; *Angew. Chem.* **2014**, *126*, 1061–1065; b) T. Kitao, S. Bracco, A. Comotti, P. Sozzani, M. Naito, S. Seki, T. Uemura, S. Kitagawa, *J. Am. Chem. Soc.* **2015**, *137*, 5231–5238.
- [17] L. D. Gong, Z. Z. Yang, *J. Comput. Chem.* **2010**, *31*, 2098–2108.
- [18] W. Zhu, F. Kapteijn, J. A. Moulijn, J. C. Jansen, *Phys. Chem. Chem. Phys.* **2000**, *2*, 1773–1779.

Received: August 8, 2016

Published online: September 28, 2016